Model Order Selection for LASSO Fitted Millimeter Wave Vehicular Channel Data

Thomas Blazek*, Erich Zöchmann*†‡, and Christoph F. Mecklenbräuker*
†Christian Doppler Laboratory for Dependable Wireless Connectivity for the Society in Motion
*Institute of Telecommunications, TU Wien, Austria
‡Department of Radio Electronics, TU Brno, Czech Republic

***Abstract*—For analysis of vehicle-to-vehicle (V2V) communications, a firm understanding of the underlying channel is crucial. Through spatial filtering of narrow beams millimeter wave (mmWave) channels become sparse. As accurate channel models are required, without overfitting channel measurements, we investigate the optimal model order given V2V mmWave channel measurements. We use the complex Least Absolute Shrinkage and Selection Operator (LASSO) to find a sparse tapped-delay line representation of the measured channel, and apply the Akaike Information Criterion to find the optimal model order. Beyond this optimal order we start to fit measurement noise. Our results show, that for the given measurements, 4 to 8 taps prove to be an ideal model order.**

***Index Terms*—mmWave, Vehicular Channel Models, c-LASSO**

I. Introduction

While vehicle-to-anything (V2X) communication has been a research focus for several years now, the market is slow in accepting the new technology. With the advent of the 5th generation of mobile telephony, millimeter wave (mmWave) communications is expected to augment the vehicular communication scenario and act as technology driver [1]. However, the vehicular channel is a challenging communication environment, as large delay and Doppler spreads are typically expected [2]. The Doppler effect scales linearly with the carrier frequency, which leads to large RMS Doppler spreads when omni-directional antennas are employed. The RMS Doppler spread is drastically reduced, if at least one link end performs beamforming [3]. Furthermore, the larger Doppler effect at mmWaves can also be useful for tracking multipath components (MPCs) [4]. mmWave channels have been shown to have a sparse structure, and the large bandwidth allows to resolve MPCs that used to be seen as fading [5]. Since an investigation of V2X communications requires a thorough understanding of the vehicular channel, knowledge of the expected complexity is of high importance. Furthermore, in vehicular settings, prototype tests under lab conditions are essential to evaluate hardware. Therefore, there is a need for representative channel models that are implementable on hardware emulators [6], [7]. The authors of [8] used sparse techniques to estimate a mmWave indoor channel, suggesting that a similar approach can work on outdoor channels. Extensive outdoor measurements have been reported in [9]. They were however not specific to V2X scenarios. Furthermore, no systematic analysis on the model order that is required to capture the channel has been conducted to the best of our knowledge.

The main contribution of this paper is to present an estimate for an optimal model order for V2V overtaking scenarios in mmWave communications. The results are based on the vehicle-to-vehicle (V2V) mmWave measurements conducted in Vienna [10], and apply (sequential) sparse estimation techniques [11] to find a sparse impulse response estimate. Then, we apply the Akaike Information Criterion (AIC) to find an optimal tradeoff between improving the mean squared error (MSE) estimate and increasing the model order. Sparse estimates are of high importance as they demonstrate the complexity-fidelity tradeoff that is essential to know for hardware and software models of such a channel.

II. Vehicular Channel Measurements

Our measurement setup is described in detail in [10]. Using an approximately 500 MHz wide multitone sequence with 5 MHz tone-spacing centered at 60 GHz, the time-variant transfer function $\mathbf{h}[i]$ is estimated. In order to achieve very accurate frequency and time synchronization, we keep RX and TX static and connected both with a 10 MHz frequency reference and a trigger cable. A measurement is triggered once an overtaking vehicle of the ordinary street traffic drives through a light barrier. This light barrier is placed in front of the receiver car. We hence observe mmWave channels where a vehicle is already passed by. To capture the effect of beamforming, a 20 dBi horn antenna is employed at TX and an open-ended waveguide with approximately 7 dBi gain is employed at RX.

III. Channel Estimation

We estimate the channel as a sparse, time-variant tapped delay line model

$$x[i,\tau] = \sum_{i=1}^{K_0} x_k[i]\delta(\tau - \tau_k[i]). \tag{1}$$

We assume the channel to have exactly K_0 active taps, and each tap is assigned a complex-valued, time-variant

Fig. 1. Photographs of the measurement site. The upper photo shows the transmit horn antenna mounted on a tripod. As multiple reflection with the transmitter car are below our receiver sensitivity, the TX car is replaced with a tripod. The lower photo shows the open-ended waveguide receive antenna mounted at roof height on a car side window.

channel coefficient $x_i[i]$, as well as a delay $\tau_k[i]$ which itself depends on the absolute time i. The length of the whole channel (impulse response) is denoted by N, where $K_0 \ll N$. For ease of notation, we we will write $x[i,\tau]$ as a vector $\mathbf{x}[i]$ of length N, that has K_0 nonzero entries. Thus, the chosen delays are encoded in the position of the nonzero values. Given noisy ($\mathbf{n}[i]$) frequency-domain measurements $\mathbf{h}[i] \approx \mathbf{F}\mathbf{x}[i] + \mathbf{n}[i]$, our goal is to find the optimal choice of the parameters x_k, τ_k for all times i to model the given measurement. The number of active taps K_0 shall remain a design parameter. This class of problems is solved by the complex Least Absolute Shrinkage and Selection Operator (c-LASSO) [11]. It has been applied to multi-slope path loss fitting [12], to direction of arrival estimation [11], [13] or to sparse channel estimation directly [14], and optimizes the following expression

$$\mathbf{x}_{\text{opt}}[i] = \arg\min_{\mathbf{x}} \left(||\mathbf{S}\,(\mathbf{h}[i] - \mathbf{F}\mathbf{x})\,||_2^2 + \mu||\mathbf{D}\mathbf{x}||_1 \right). \quad (2)$$

Here, $||\cdot||_p$ denotes the p-norm, $\mathbf{F}$ is the centered unitary discrete fourier transform (DFT) of size N and $\mathbf{S}$ allows to calulate a weighted MSE. This objective function attempts to minimize the MSE, but by adding the 1-norm through the Lagrangian multiplier μ, a small number of nonzero entries are favored. The diagonal weighting matrix $\mathbf{D}$ allows to adjust sparseness penalties for different entries of $\mathbf{x}$. Following the algorithm from Table 3 in [11], the impulse response estimate $\mathbf{x}_{\text{opt}}[i]$ with the desired sparseness K_0 is found.

The results from the algorithm will be compared to the results from *peak search*. In peak search, we first compute the dense impulse response $\mathbf{x}' = \mathbf{F}^H\mathbf{h}$. Then, we establish the delays by finding the K_0 strongest peaks in $\mathbf{x}'$. Finally, we construct the tall DFT matrix $\mathbf{F}' \in \mathbb{C}^{N\times K_0}$, and compute the peak search estimate through the Moore-Penrose pseudoinverse $(\cdot)^\dagger$ to $\mathbf{x}_{\text{peak}} = \left(\mathbf{F}'\right)^\dagger\mathbf{h}$. In the following sections, we will present two ways of choosing the $\mathbf{D}$ and $\mathbf{S}$ matrices, and how the choices impact the results.

A. Estimation Strategies

We propose to use sequential estimation to limit instantaneous births and deaths of channel taps due to noise fitting. As reference, we provide results for memoryless estimation as in [14].

1) Memoryless Estimation: In the memoryless case we choose $\mathbf{D}$ to be an identity matrix of size $N \times N$. Thus, for every new time step i, a new estimate $\mathbf{x}[i]$ is calculated that is independent of past estimates, and all possible taps are equally weighted. Additionally, we consider three different bandwidths of interest: the full measurement bandwidth (500 MHz), half the bandwidth (250 MHz), and quarter the bandwidth (125 MHz). Within the bandwidth of interest, we do however weigh the frequencies equally in the MSE. Thus, $\mathbf{S}$ is constructed as

$$\mathbf{S} = \text{Diag}\left(\begin{bmatrix} \mathbf{0}^{1\times(N-N_s)/2} & \mathbf{1}^{1\times N_s} & \mathbf{0}^{1\times(N-N_s)/2} \end{bmatrix} \right). \quad (3)$$

The operator Diag$(\cdot)$ constructs a diagonal matrix where the diagonal equals the given vector, and N_s is the number of frequency samples corresponding to our chosen bandwidth. Since the LASSO algorithm aims for sparse fits, it does not converge well in non-sparse scenarios, thus we will only consider model orders that suffice $\frac{K_0}{N_s} < 0.25$.

2) Sequential Estimation: The main drawback of the memoryless approach is that it does not account for the underlying physics. If a dominant scatterer is known to

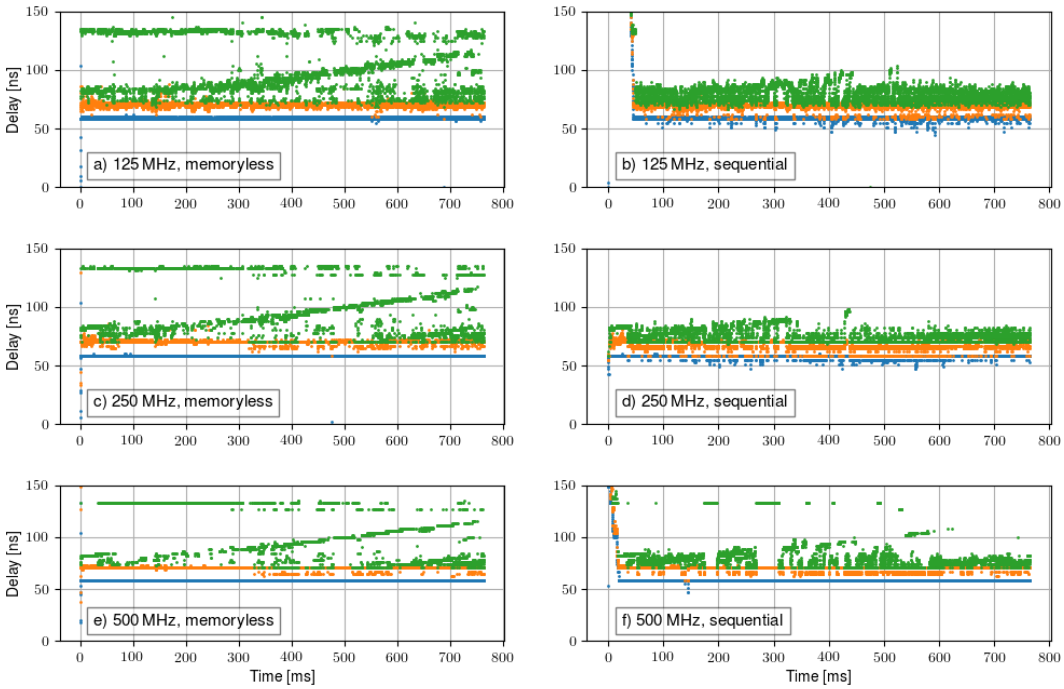

Fig. 2. 3-tap delay evolution for an overtaking truck. First tap in blue, second tap in orange, and third tap in green.

have a given propagation delay, this delay cannot change inconsistently with the geometry.

Since measurements are noisy, the tap positions may vary from snapshot to snapshot because the algorithm fits noise. Therefore, we introduce a sequential evolution imposing a structure on $\mathbf{D}$, that is derived from [13]. The weight matrix $\mathbf{D}[0]$ is initialized as identity matrix like in the memoryless case. Then, for all timesteps, the following rules are applied

a) Propagation of active taps: A scatterer can physically move at most 1 delay sample (2 ns, 4 ns, or 8 ns for the respective bandwidths) between two snapshots. Thus, after calculating an estimate $\mathbf{x}[i]$, we adapt

$$D_{j,j}[i+1] = \left(\sum_{k=j-1}^{j+1} D_{k,k}[i]^{-2} \right)^{-1} \tag{4}$$

for all j that are within 1 tap of at least 1 nonzero entry of $\mathbf{x}[i]$. This will always lower the entry in the diagonal, making it less penalized in the optimization, and thus more likely to be picked again.

b) Discouraging spawning new taps: For all entries that were not modified in the previous step, we apply

$$D_{j,j}[i+1] = D_{j,j}[i] + 0.1. \tag{5}$$

This ensures that scarcely activated taps get progressively penalized, ensuring that random noise is less likely to activate such a tap. Finally, all diagonal entries below 10^{-4} are set to 10^{-4} to ensure computational stability.

B. Estimation Output

The estimated delays for 3 active taps are shown in Figure 2 for an overtaking truck, and Figure 3 for an overtaking SUV. We use 3 taps for demonstration purposes to ensure the visual clarity of the figures here. The memoryless estimation results in the taps being randomly spread until approximately 300 ms. Increasing the bandwidth leads generally to fewer fluctuations. The sequential estimation reduces these random fluctuations. However, the output shows that choosing the correct weights is not trivial and has to be investigated further. Graphically the sequential estimation works better for the SUV measurement.

IV. Model Order Selection

We will now investigate the optimal model order given the bandwidth of interest. To this end, we introduce our performance metrics, and analyze the results.

A. Performance Metrics

We define the MSE as dependent on the bandwidth of interest

$$\text{MSE} = \frac{||\mathbf{S}(\mathbf{h} - \mathbf{F}\mathbf{x})||_2^2}{N_S}. \tag{6}$$

Since we are accounting for the weighting matrix in the MSE, we are able to directly compare the MSEs of different bandwidth optimizations.

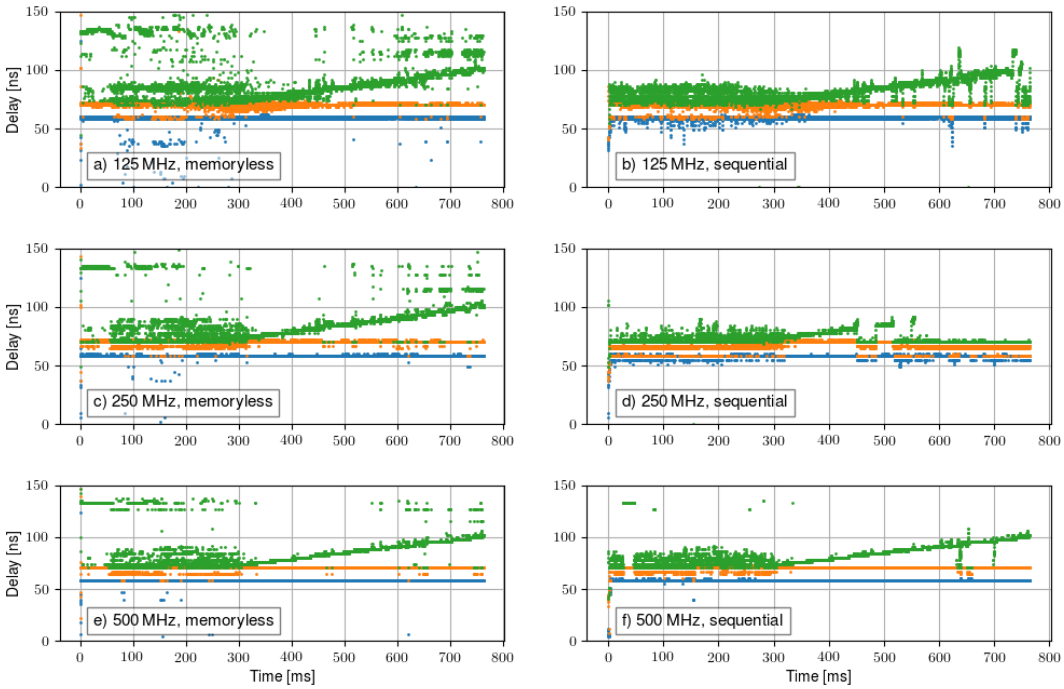

Fig. 3. 3-tap delay evolution for an overtaking SUV. First tap in blue, second tap in orange, and third tap in green.

However, the MSE is ill-equipped to tackle the question of overfitting, as it does not penalize increasing the model order, and thus always favors higher model order over lower. An important measure that is able to capture the effect of overfitting is the Akaike Information Criterion (AIC), which is, for linear regression of Gaussian data, defined as [15]

$$\mathrm{AIC} = N_s \ln(\mathrm{RSS}) + 2k \ . \tag{7}$$

RSS denotes the residual sum of squares $\mathrm{RSS} = ||\mathbf{S}(\mathbf{h} - \mathbf{F}\mathbf{x})||_2^2$, and N_s denotes the number of estimated frequency samples. Figure 4 shows that the assumption of Gaussian data is founded, as real and imaginary part of the channel parameters are well fitted by a Gaussian distribution. Due to the nonlinear structure of the AIC, results based on different numbers of subcarriers are not directly comparable, as it considers N_s variables being fitted by k parameters.

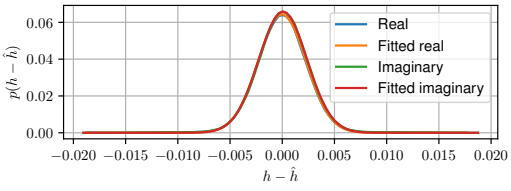

Fig. 4. Distribution of the estimation error.

B. Results

Figure 5 shows the MSE and AIC for a truck measurement and Figure 6 for an SUV measurement. As a reference, the results for peak search are shown. The MSE results demonstrate that limiting the model bandwidth progressively improves the estimation quality. This is not surprising, as effectively a higher ratio of taps per estimated frequency samples are used. However, we do point out that the 125 MHz estimation behaves especially well, reaching MSE values at 4 taps that the other estimates only reach at more than 15 taps. Larger bandwidths will split single taps into a cluster of multiple taps, so that the estimation quality in terms of MSE worsens. This behavior is also demonstrated in [16], where a similar approach is conducted on parallel subbands to span a larger bandwidth. On the other hand, the model order selected by the AIC is very stable over bandwidth. The AIC shows through the local minimum what number of coefficients have the best trade-off between model order and MSE fit. We conclude that smaller vehicles, such as SUVs or cars, are best modeled with 4 taps and larger vehicles, such as trucks or buses, are best modeled with 6-8 taps. Furthermore, we see a gap in MSE (and hence also in the absolute AIC value) between memoryless and sequential estimation. This is to be expected, since the cost function of the sequential estimation combines the MSE of the current observation and the concordance to the history.

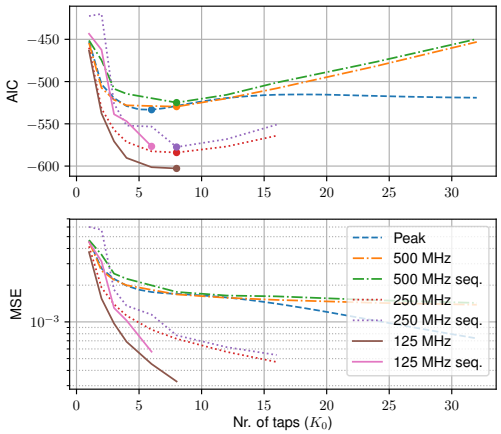

Fig. 5. MSE and AIC of a truck measurement. Dots illustrate the minima of the AIC.

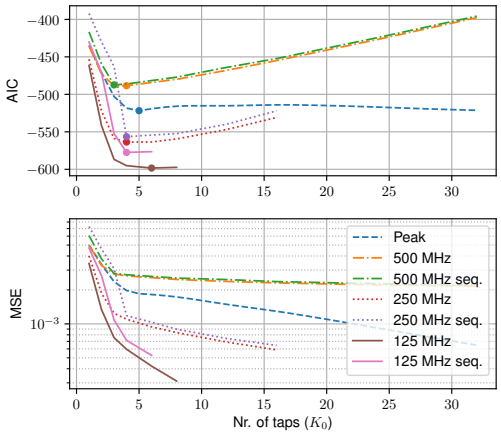

Fig. 6. MSE and AIC of a cross-polarized measurement.

V. Conclusion

We analyze the complexity of the millimeter wave V2V channel for an overtaking scenario, and demonstrate that the model quality strongly depends on the target model bandwidth. On the other hand, regardless of the chosen bandwidth, our results show a dominance of few scattering objects. This is underlined by the AIC analysis, which shows optimal fitting orders between 4 and 8 taps. Higher tap numbers are suggested to be overfitting, and likely fit measurement noise. Thus, when modeling a mmWave channel, careful choice of the required bandwidth is essential, while few multipath components are required. For channel emulation applications, this translates to simple implementations, as long as the hardware requirements are met.

Acknowledgements

The financial support by the Austrian Federal Ministry of Science, Research and Economy and the National Foundation for Research, Technology and Development is gratefully acknowledged. The research has been co-financed by the Czech Science Foundation, Project No. 17-18675S "Future transceiver techniques for the society in motion", and by the Czech Ministry of Education in the frame of the National Sustainability Program under grant LO1401. This work was partially funded by Austrian Development Cooperation and Ministry of Education, Science and Technology of Republic of Kosovo, in the framework of the project HERAS K-01-2017 as research cooperation and networking between Austria, Kosovo and the Western Balkan Region.

References

[1] J. Choi, V. Va, N. Gonzalez-Prelcic, R. Daniels, C. R. Bhat, and R. W. Heath, "Millimeter-wave vehicular communication to support massive automotive sensing," *IEEE Communications Magazine*, vol. 54, no. 12, pp. 160–167, December 2016.

[2] C. F. Mecklenbräuker, A. F. Molisch, J. Karedal, F. Tufvesson, A. Paier, L. Bernado, T. Zemen, O. Klemp, and N. Czink, "Vehicular Channel Characterization and Its Implications for Wireless System Design and Performance," *Proc. IEEE*, vol. 99, no. 7, pp. 1189–1212, Jul 2011.

[3] Zöchmann *et al.*, "Statistical evaluation of delay and Doppler spread in 60 GHz vehicle-to-vehicle channels during overtaking," in *Proc. IEEE APWC*, 2018.

[4] E. Zöchmann, S. Caban, M. Lerch, and M. Rupp, "Resolving the angular profile of 60 GHz wireless channels by delay-Doppler measurements," in *Proc. of IEEE Sensor Array and Multichannel Signal Processing Workshop (SAM)*, 2016.

[5] C. Gustafson, K. Haneda, S. Wyne, and F. Tufvesson, "On mm-wave multipath clustering and channel modeling," *IEEE Transactions on Antennas and Propagation*, vol. 62, no. 3, pp. 1445–1455, Mar 2014.

[6] M. Hofer, Z. Xu, and T. Zemen, "Real-time channel emulation of a geometry-based stochastic channel model on a SDR platform," in *Proc. of IEEE 18th SPAWC*, 2017, pp. 1–5.

[7] G. Ghiaasi, T. Blazek, M. Ashury, R. R. Santos, and C. Mecklenbräuker, "Real-time emulation of nonstationary channels in safety-relevant vehicular scenarios," *Wireless Communications and Mobile Computing*, vol. 2018, 2018.

[8] R. He, W. Chen, B. Ai, A. F. Molisch, W. Wang, Z. Zhong, J. Yu, and S. Sangodoyin, "On the clustering of radio channel impulse responses using sparsity-based methods," *IEEE Transactions on Antennas and Propagation*, vol. 64, no. 6, pp. 2465–2474, June 2016.

[9] T. S. Rappaport, G. R. MacCartney, M. K. Samimi, and S. Sun, "Wideband millimeter-wave propagation measurements and channel models for future wireless communication system design," *IEEE Transactions on Communications*, vol. 63, no. 9, pp. 3029–3056, Sept 2015.

[10] E. Zöchmann *et al.*, "Measured delay and Doppler profiles of overtaking vehicles at 60 GHz," in *Proc. of the 12th European Conference on Antennas and Propagation (EuCAP)*, 2018.

[11] C. F. Mecklenbräuker, P. Gerstoft, and E. Zöchmann, "c–LASSO and its dual for sparse signal estimation from array data," *Signal Processing*, vol. 130, pp. 204–216, 2017.

[12] E. Zöchmann, K. Guan, and M. Rupp, "Two-ray models in mmWave communications," in *Proc. of IEEE 18th International Workshop on Signal Processing Advances in Wireless Communications (SPAWC)*, 2017.

[13] E. Zöchmann, P. Gerstoft, and C. F. Mecklenbräuker, "Density evolution of sparse source signals," in *Proc. of 3rd Int. Workshop on Compressed Sensing Theory and its Applications to Radar, Sonar and Remote Sensing (CoSeRa)*, 2015, pp. 124–128.

[14] T. Blazek and C. Mecklenbräuker, "Sparse time-variant impulse response estimation for vehicular channels using the c-LASSO," in *Proc. 2017 IEEE 28th PIMRC*, Oct 2017.

[15] K. P. Burnham and D. R. Anderson, "Multimodel inference: understanding AIC and BIC in model selection," *Sociological methods & research*, vol. 33, no. 2, pp. 261–304, 2004.

[16] T. Blazek, E. Zöchmann, and C. Mecklenbräuker, "Approximating clustered millimeter wave vehicular channels by sparse subband fitting," in *Proc. 2018 IEEE 29th PIMRC*, Bologna, Italy, Sep. 2018.